EPDM−Carbon Black Interactions and the Reinforcement Mechanisms, As Studied by Low-Resolution ^{1}H NMR

V. M. Litvinov* and P. A. M. Steeman

DSM Research, PAC-MC, P.O.Box 18, 6160 MD Geleen, The Netherlands

Received June 24, 1999

ABSTRACT: Proton, low-resolution T_2 NMR relaxation experiments are used to study the adsorption of EPDM to the surface of carbon blacks and the structure of the physical EPDM/carbon black network in cured and uncured compounds. It is shown that a layer of immobilized EPDM is formed at the carbon black surface after mixing. The estimated thickness of the interfacial EPDM is in the range of one to two diameters of the monomer unit (≈1 nm). At temperatures of up to 160 °C, the mobility of EPDM chain units in the interface is strongly hindered and is comparable to that in an unfilled EPDM at temperatures 10−15 deg above T_g. It is suggested that the sites of the interaction between the carbon black and the EPDM cause physical adsorption network junctions in the rubber matrix. The average molar mass of EPDM chains between the adjacent adsorption junctions in bound EPDM rubber is about 1800−2500 g/mol and depends on the content and the type of the filler. The mean end-to-end distance between the adsorption junctions is comparable to the average distance between the adjacent carbon black aggregates. This suggests that the carbon black aggregates are interconnected by EPDM bridging chains, and a continuous EPDM/carbon black physical network is formed in the bound rubber fraction of the compound. The results obtained for uncured filled rubbers provide strong evidence of a "bimodal" structure of the physical network. The two types of EPDM chains and/or chain fragments, which have strongly different densities of EPDM−carbon black adsorption junctions, are present in the elastomer matrix outside of the *EPDM−carbon black interface*. There is an EPDM fraction that is *loosely bound* to the carbon black by adsorption interactions. This loosely bound rubber has numerous adsorption network junctions, similar to those of the bound rubber. The other fraction of EPDM, *the extractable (unbound) rubber*, has a relatively low number of adsorption network junctions and can apparently be extracted from the compound. The fraction of loosely bound EPDM chains, as measured by NMR, increases as the maximum possible EPDM−carbon black contact area per unit volume of the elastomer increases, regardless of the type of carbon black, and is relatively close to the content of the bound rubber. Results of mechanical property tests on the carbon black filled vulcanisates reveal that several factors contribute to the reinforcing effect of the filler. Besides the hydrodynamic effects, the occluded EPDM, the chemical cross-links, and the formation of the physical EPDM−carbon black network, the filler−filler interactions provide a significant contribution to the modulus in the low-strain region, while they are broken at high strains.

Introduction

The incorporation of carbon black into a rubber, for instance an EPDM, is of significant commercial importance, since carbon black not only enhances the mechanical properties of the final products but also decreases the cost of the end product. Despite numerous investigations on carbon black filled rubbers using different techniques, the molecular origin of the reinforcement effect is still under discussion.[1−9] It is generally believed that the nature of the elastomer−filler interactions is of major importance for the improvement of the mechanical properties of filled rubbers at a high elongation. The reinforcement at a moderate strain (<7%) is greatly affected by a disruption of the continuous network of filler which interpenetrates the rubber matrix.[9] The elastomer−filler interactions are often characterized by the content of the apparent "bound" rubber, which is determined as the amount of insoluble rubber adhering to the dispersed carbon black aggregates before vulcanization.[10] Since the amount of bound rubber is related to the surface area and the surface activity of carbon blacks, it is widely accepted that this phenomenon is caused by a multicontact chain adsorption to the surface of the filler. A number of structure−properties relations have been established between the content of bound rubber and the mechanical properties of filled rubbers.[1,2,10−12] However, the true nature of the bound rubber is still under debate: "*The fundamental dilemma is whether it actually exists a three-dimensional network made up of fibrous elements of carbon black and bound rubber in the vulcanisate, or whether it is simply a test method dependent on known reinforcement factors. Is bound rubber indicative or operative?*".[12] Therefore, it is of great practical importance to understand the molecular structure of bound rubber.

Apparently, the elastomer−filler interactions are of great importance due to the large total elastomer−carbon black contact area. However, there is a lack of techniques that can provide information about the physical properties and the fraction of the interface between the rubber matrix and the carbon black particles in filled rubbers.

A low-resolution proton NMR method is one of the few successful techniques used for the study of elastomer−filler interactions in a carbon black filled natural rubber and a fumed silica filled silicon rubber.[13,14] According to these studies, the physical adsorption of the elastomer chains to the surface of the fillers causes a significant immobilization of the rubber chains adjacent to the filler surface. The two microregions with strongly different local chain mobility that are present

* To whom correspondence should be addressed.

10.1021/ma9910080 CCC: $18.00
Published on Web 11/20/1999

Table 1. Chemical Composition and Properties of the EPDMs

EPDM-1	composition (in mass %)	ethylene	44.6
		propylene	45.4
		ethylidene norbornene	10.0
EPDM-2			
		ethylene	46
		propylene	49
		ethylidene norbornene	5
	Mooney viscosity ML(1 + 4)125 °C		30[a]
	molar mass (×1000 g/mol)	M_n	32
		M_w	132
		M_z	517
	long chain branching parameter, $\Delta\delta$[21]		9.8

[a] Mooney units.

in the filled rubbers are the low mobile (semirigid) rubber layer, which covers the filler surface, and the elastomer matrix outside of this interface.[13] Because of the physical adsorption of the elastomer chains to the filler surface, the filler particles are "glued" in the rubber matrix. The filler aggregates, which are covered by the interface, can be considered as multifunctional, physical cross-links, which provide a significant amount of physical adsorption network junctions for the elastomer matrix.[13] The density of these physical junctions was determined for silica filled PDMS.[13,18] The NMR method has also been used for a quantitative determination of the density of chemical cross-links in unfilled and filled rubber networks[13,15−20] and chain entanglements.[20]

Proton T_2 relaxation experiments are used in the present study to investigate the following effect of carbon black on the rubber matrix in filled EPDM rubbers: (i) the EPDM/carbon black interface, (ii) the density of the adsorption junctions in the rubber matrix of a bound EPDM rubber as a function of the load and type of carbon black, (iii) the heterogeneity of the physical network structure in the rubber matrix of nonvulcanized, filled EPDM compounds as a function of the content and type of carbon black, and (iv) the network structure in carbon black filled EPDM vulcanisates filled with various amounts of carbon black and cured with the same amount of vulcanization ingredients.

Mechanical experiments are used to determine the macroscopic behavior of the filled rubbers. The results of the solid-state NMR and mechanical experiments are compared in order to evaluate the effects of the network structure, the carbon black−carbon black interaction, and the strain amplification on the rubbery properties.

Experimental Section

A. Characterization of the Initial Components. 1. EPDM. The chemical composition and the properties of EPDM rubbers that were used for the preparation of EPDM vulcanisates (EPDM-1) and raw and bound rubbers (EPDM-2) are shown in Table 1. Because of its low viscosity and broad molar mass distribution, EPDM-2 can be mixed with a large fraction of carbon black with a high specific surface.

2. Carbon Black. The carbon blacks used were rubber grade furnace black N-Vulcan 10HX132-1, Vulcan-3, and Regal SRF (ASTM codes are N110, N330, and N550, respectively) from Cabot B.V., NL. Some of the physical properties of the carbon black are listed in Table 2. *The surface area* of the carbon black used is characterized by the so-called iodine number, the value of which is usually close to the surface area of carbon black aggregates measured in m^2/g by adsorption of hexadecyltrimethylammonium bromide (CTAB method). The CTAB method determines the surface area, which is active for the elastomer chains, since the micropores are not measured by this method. *The size distribution of the carbon black particles* is characterized by a MESH number which corresponds to a sieve opening diameter: 0.50 and 0.045 mm for 35 and 325 MESH, respectively. *The degree of structure of the carbon blacks* is characterized by the *di*-butyl phthalate (DBP) adsorption method. This method measures the adsorption of DBP in the cavities (empty voids) between the carbon black aggregates in agglomerates. The smaller the particle size, the higher the DBP value. For the same surface area, a higher DBP value is observed for the carbon blacks with a higher degree of agglomeration, i.e., with stronger van der Waals forces between the carbon black aggregates. The DBP adsorption method measures the filler structure before the filler is incorporated into the elastomers. Therefore, the DBP value does not define the carbon black structures which exist in mixtures of rubbers with carbon blacks.

Table 2. Physical Properties of the Carbon Blacks

properties	test method	N550	N330	N110
iodine number, mg/g	D-1510	29.9	83.3	142.6
specific surface (CTAB), m^2/g	D-3765		83.4	
DBP adsorption, mL/100 g	D-2414	64.5	102.1	125.9
35 MESH, ppm		0	0	0
325 MESH, ppm		14	10	117

B. Preparation of Compounds. The EPDM was extensively mixed with the carbon blacks on a laboratory rolling mill at 100 °C. Repetitive cutting and milling of the rubber strips was used to ensure a good dispersion of the carbon black in the EPDM. The friction ratio used was 1:1.2. The carbon black content in the compounds was 40, 60, 85.5, and 100 mass parts per 100 mass parts of EPDM-2 (phr) according to weighting of the mixture ingredients and the thermogravimetric analysis (TGA) of the compounds. Prior to the preparation of the bound rubber and the NMR experiments, the compounds were stored at room temperature for 1 month before extraction in order to reach the equilibrium state for the adsorption of the EPDM chains.[22]

The homogeneity of the carbon black distribution was studied by transmission light microscopy on the samples with a carbon black content of 40 phr. Under deep cooling with liquid nitrogen, about 1 μm sample slices were cut on a microtome with a glass knife. Both the SFM and the optical microscopy pictures showed a fairly good dispersion of the carbon black on a micrometer scale. Nevertheless, the compounds filled with N110 and N550 contained on average from 2 to 3 large carbon black agglomerates per 0.3×10^{-4} mm^3 volume of the samples. The size of these agglomerates was about 10−30 μm.

The volume fraction of the carbon black in the samples, φ, was calculated for the specific density of EPDM and the carbon black of 0.86 and 1.85 g/cm^3, respectively.[1,11] The filler surface area per unit volume of EPDM is represented by a value of $(\varphi\rho S_{sp})/(1 - \varphi)$, where ρ and S_{sp} are the specific density and the specific surface of carbon black, respectively. This value is expressed in m^2 of the carbon black surface per cm^3 of EPDM. The mean distance between the carbon black aggregates, δ_{aa}, was estimated using the equation[23]

$$\delta_{aa} = (6000/\rho S_{sp})(k\varphi^{-1/3}\beta^{-1/3} - 1)\beta^{1.43} \quad (1)$$

where k is a constant, the value of which depends on the type of packing of the carbon black aggregates. For random packing, k is about 0.85. The value of β is the ratio of the effective volume fraction of a carbon black in a rubber, φ_{eff}, to the actual volume fraction φ. For the random packing of equivalent spheres, β is determined by the equation[23]

$$\beta = \varphi_{eff}/\varphi = [0.0181(\mathrm{DBPA}) + 1]/1.59 \quad (2)$$

Table 3. Characteristics of the Compounds

compound[a]	φ	$(\varphi\rho S_{sp})/(1-\varphi)$, m^2_{CB}/cm^3_{EPDM}	δ_{aa}, nm
N550/40	0.157	10.3	71
N550/60	0.218	15.4	46
N550/85.5	0.284	22.0	28
N550/100	0.317	25.7	21
N330/40	0.157	28.7	27
N330/60	0.218	43.0	15
N330/85.5	0.284	61.2	5.8
N330/100	0.317	71.6	2.3
N110/40	0.157	49.0	15
N110/60	0.218	73.6	7.0
N110/85.5	0.284	104.8	1.0

[a] The compounds are designated by the two numbers which represent the type of the carbon black according to the ASTM codes and its content in parts by weight of filler per 100 parts by weight of the rubber (phr).

where DBPA is the DBP adsorption number for a carbon black.

These characteristics of the compounds are given in Table 3.

C. Preparation of the Bound Rubber. According to previous studies,[8,12] the amount of bound rubber depends on the quality of the solvent used for the extraction as well as on the time and the temperature of extraction. The solvents with stronger specific interactions with the carbon blacks cause a decrease in elastomer adsorption, which results in a decrease in the amount of bound rubber. Therefore, the following three different extraction sets were used for each sample: extraction with *n*-hexane (HE), with a mixture of *o*-xylene with 2 wt % of acetonitrile (X/AN), and with *n*-hexane in an ammonia atmosphere (HE/N), as described below. The choice of the different solvents was based on the different abilities of the solvents to form hydrogen bonds and π-bonds with the adsorption sites on the surface of the carbon black. Acetonitrile and ammonia show a high ability to form hydrogen bonds with the polar groups on the surface of the carbon black. It appears that *o*-xylene is capable of forming only the conjugated π-bonds with the carbon atoms at the crystallite edges from the quasi-graphitic layers on the surface of the carbon black.

The rubbers were cut into approximately 1 mm^3 pieces. About 4 g of the rubber was subsequently immersed in 50 mL of a solvent. The extraction was carried out for 80 days at room temperature. For the HE/N extraction, the uncovered bottles with swollen rubbers were placed in a flask with a water solution of ammonia at the bottom. Then the flask was closed with a stopper. To prevent a possible degradation of the rubbers, 0.1 wt % of a stabilizer, 2,6-*di*-*tert*-butyl-*p*-cresol (DTPC), was added to the solvents. The swollen rubber gels were decanted every 5 days, and a fresh solvent was added. After the extraction was finished, the swollen rubber gels, the bound rubber, were decanted and were immersed twice for 1 h in $C_2H_2Cl_2$, to replace less volatile solvents with $C_2H_2Cl_2$, which has a lower boiling point (40 °C). Afterward, the bound rubbers were dried for 1 day in air at room temperature and then for 14 days in an oven at 120 °C in a vacuum of 5 mbar. At the end, the samples were held in a vacuum of 7×10^{-1} mbar for 450 min at 140 °C. A small flow of nitrogen was used during drying. The respective amounts of the EPDM and the carbon black in the bound rubbers were determined by TGA. The TGA experiment combined with a mass spectrometric analysis showed that there were no residual solvents in the dried bound rubbers, but the samples still contained about 0.1−0.6 wt % of adsorbed water after having been exposed to humid air.

The EPDM/N110 compound (phr = 85.5) was also extracted in boiling *o*-xylene for 8 h in the presence of DTPC as a stabilizer. After the extraction, the rubber gel was dried in an oven at 120 °C in a vacuum of 5 mbar, until the sample weight remained constant in time.

The fraction of the apparently bound rubber, R_b, was determined as the weight of EPDM in the gel after extraction relative to the weight of EPDM in the compound. The average thickness of the bound layer, R_0, was calculated assuming that a uniform layer of the bound rubber covers the complete surface of the carbon black. The characterization of the bound rubbers is given in Table 4.

Table 4. Characteristics of the Bound Rubber

compound[a]	solvent	R_b, %	φ	$(\varphi\rho S_{sp})/(1-\varphi)$, m^2_{CB}/cm^3_{EPDM}	R_0, nm
N550/60	HE	8.5	0.767	182	5.49
	X/AN	8.2	0.773	188	5.32
	HE/N	7.9	0.780	196	5.11
N550/100	HE	13.1	0.775	191	5.24
	X/AN	12.7	0.786	203	4.93
	HE/N	13.3	0.777	193	5.18
N330/40	HE	16.2	0.535	177	5.64
	X/AN	15.7	0.542	182	5.48
	HE/N	16.2	0.534	177	5.67
N330/60	HE	23.2	0.546	185	5.40
	X/AN	23.1	0.547	186	5.38
	HE/N	23.5	0.542	183	5.48
N330/85.5	HE	29.5	0.574	208	4.82
	X/AN	29.6	0.573	207	4.84
	HE/N	29.9	0.571	205	4.88
N330/100	HE	32.4	0.589	221	4.52
	X/AN	34.9	0.571	205	4.87
	HE/N	32.9	0.586	218	4.59
N110/40	HE	23.7	0.440	207	4.83
	X/AN	22.7	0.451	217	4.62
	HE/N	24.5	0.431	200	5.00
N110/60	HE	32.4	0.462	227	4.41
	X/AN	31.5	0.471	235	4.26
	HE/N	33.5	0.454	219	4.56
N110/85.5	HE	37.7	0.511	276	3.63
	X/AN	40.6	0.495	258	3.87
	HE/N	37.8	0.515	280	3.57
	boiling *o*-xylene	39.1	0.504	268	3.73

[a] The compounds are designated by the two numbers which represent the type of the carbon black according to the ASTM codes and its content in parts by weight of filler per 100 parts by weight of the rubber (phr).

D. Preparation of the EPDM Vulcanisates. The EPDM vulcanisates containing a different amount of carbon black N550 were prepared from the EPDM-1 by sulfur vulcanization. The recipe contains sulfur (1.88 phr), zinc oxide (5 phr), stearic acid (1 phr), mercaptobenzothiazole (0.63 phr), and tetramethylthiuram disulfide (1.25 phr). The vulcanisates were prepared by compression molding at 160 °C/30 min, using 2 mm press plates.

E. Preparation of the Swollen Samples. A number of samples were studied in the swollen state. A certain amount of C_2Cl_4 was added to a sample. A sample tube was tightly closed with a Teflon cylinder, the bottom part of which was slightly above the upper part of the sample. The volume fraction of EPDM, V_p, in the swollen samples was varied from 1 to 0.135. A value of V_p for the filled samples was determined as the ratio of the volume of the dry gel to the volume of the swollen gel. The volume of the carbon black was subtracted for the calculation of the V_p value.

F. Solid-State NMR Experiments and Data Analysis. 1. Equipment. Proton T_2 relaxation experiments were performed on a Bruker Minispec PC-120 spectrometer at a proton resonance frequency of 20 MHz. This spectrometer was equipped with a home-built variable temperature unit. Dry nitrogen was used for cooling or heating the samples. The temperature gradient and stability was about 1 °C.

2. Measurement of the Decay of the Transverse Magnetization. Several precautions have to be taken to accurately measure the transverse magnetization decay for (micro)-heterogeneous materials containing both low mobile and highly mobile fractions. *The errors cannot practically be eliminated, but their effects can be minimized to a large extent.* Two different pulse sequences have to be used in order to obtain T_2 values for both (micro)regions as well as for the rigid/mobile ratio.

The solid-echo pulse sequence, SEPS ($90°_x-\tau-90°_y-\tau-$acq), with $\tau = 20$ μs was used to record the magnetization of the low mobile fraction of the rubbers. The echo decay was recorded starting from the echo maximum, time $t = 0$. The SEPS has the advantage of avoiding the "dead" time of a spectrometer. The T_2 relaxation time below about 100 μs was measured by this pulse sequence. However at $t > 200$ μs, the SEPS does not eliminate the effect of the inhomogeneity of the magnetic field B_0 itself and the large inhomogeneity of B_0 within a sample volume, which arises from an inhomogeneous magnetic susceptibility of the heterogeneous samples. For this reason, the SEPS cannot be used for an accurate determination of the T_2 relaxation times longer than about 100 μs.

The Hahn-echo pulse sequence, HEPS ($90°_x-\tau'-180°_x-\tau'-$acq), was used to measure the transverse magnetization of the mobile region only. At $\tau' > 50$ μs, the magnetization of the low mobile fraction of the rubber vanishes, the second pulse in the HEPS inverts the nuclear spins in the mobile region of a sample, and an echo signal is formed with a maximum at time $t = 2\tau'$ after the first pulse. By varying the pulse spacing in the HEPS, the amplitude of the transverse magnetization is measured as a function of time $2\tau'$. The HEPS makes it possible to eliminate the magnetic field B_0 and the chemical shift inhomogeneities and to accurately measure the T_2 relaxation time for the mobile region only.

Thus, both the SEPS and the HEPS experiments have to be used for an accurate study of both the low mobile and the highly mobile regions in heterogeneous polymers. In the time interval from about 50 to 100−200 μs, both the SEPS and the HEPS provide relatively accurate values for the magnitude of the transverse magnetization. The decay of the transverse magnetization for bound rubber was constructed from the data points which were measured by the SEPS and the HEPS in a time domain ranging from 0 to 100 μs and above 68 μs for the SEPS and the HEPS, respectively. The combined decays were used to determine the contents of the low mobile region. It should be noted that the rigid/mobile ratio measured can be somewhat lower than its actual value due to a rather long 2τ value used in SEPS, which results in a relative decrease in the intensity of the fast decaying component.

3. Analysis of the Decay of Transverse Magnetization. All decays of the transverse magnetization were analyzed using nonlinear, least-squares adjustment of the parameters of an optional decay function, such as an exponential function, a Weibull function, a normal and a log-normal distribution of exponents, and a function that was suggested by Cohen-Addad for elastomeric networks and is hence referred to as the Cohen-Addad function.[24] The fitting program was written at DSM and employs the Levenberg−Marquardt algorithm.[25] The time constant of the above functions is represented by the T_2 relaxation time. In cases in which the transverse magnetization decay was composed of discrete relaxation components with a strongly different decay time, a linear combination of the functions was used to describe the decay. Such an analysis assumes that polymer chains and/or chain segments of different mobility are present in a sample. In most cases, the T_2 values given below are the averages of the values that were calculated using a number different models. The maximum deviation of the particular values from the mean value usually did not exceed 5%. The precision of the T_2 experiments is 2%. The correlation matrix, the Mallow's C_p parameter, and the Z values were used to statistically justify the relevance of the fits.[25]

G. Mechanical Experiments. The low-strain mechanical properties of the vulcanized samples with 0−100 phr carbon black N550 were determined by dynamic mechanical measurements[26] in tension using a Rheometric Scientific RSA-2 dynamic mechanical analyzer. Temperature sweeps were performed in the temperature interval between −100 and +100 °C with a fixed frequency of 1 Hz. Care was taken that the maximum applied strain did not exceed the linear viscoelastic range. From these results the storage modulus (E') in the glassy state (at −75 °C, i.e., 25−30 °C below the glass transition temperature at 1 Hz) and in the rubbery state (at +30 °C, i.e., 70−80 °C above the glass transition temperature at 1 Hz) was extracted for various samples. These values were used in the data evaluation. The reinforcing factor (f) of the filler particles was calculated using the modulus values of the unfilled sample as a reference.

Additionally, the high-strain mechanical properties were studied using the Mooney-Rivlin method.[27] For this purpose tensile measurements were performed with a Zwick 1474 tensile tester at room temperature. The samples, with a grip length of 50 mm and a l_0 of 20 mm, were stretched at a cross-bar speed of 15 mm/min. After stretching to 200%, the samples were unloaded. Next, the measurement was repeated. The results of the second experiment were used for a so-called Mooney-Rivlin analysis:

$$\frac{\sigma}{\lambda - 1/\lambda^2} = 2C_1 + 2C_2/\lambda \qquad (3)$$

in which σ is the stress, λ ($=l/l_0$) is the elongation of the sample, and C_1 and C_2 are the well-known Mooney-Rivlin constants. The value of $2C_1 + 2C_2$, a measure of the cross-link density in unfilled systems, is used in the data evaluation. Again, the reinforcing factor (f) of the filler was calculated using the $2C_1 + 2C_2$ value of the unfilled sample as reference.

H. Scanning Force Microscopy. The contact SFM micrographs were obtained with a Nanoscope III (Digital Instruments) on cryocut samples. Prior to cutting, the samples were embedded in the epoxy matrix. The following sample preparation was used for the experiment. To prepare a flat and clean surface, the compounds were pressed against a glass substrate at 130 °C. Three types of SFM images were used, i.e., topography, amplitude, and phase. SFM was operating in the tapping mode at a resonance frequency of ≈360 kHz and using Si probes with a spring constant of ≈50 N/m.

I. NMR Study of Molecular Scale Heterogeneity in Filled Rubbers. 1. Types of Heterogeneity in Filled Rubbers. Carbon black filled rubbers have a very complex morphology. The molecular scale heterogeneity of the rubber matrix can be due to the following reasons:

(i) The chemical heterogeneity of unfilled elastomers. The following types of "chemical" heterogeneity are present in nonvulcanized EPDMs: molar mass distribution, chain branches and chain sequences of different microstructure in the terpolymers, network heterogeneity. The effect of molar mass distribution and long chain branches on the properties is reduced in filled rubbers and vulcanisates for small network mesh sizes.

(ii) A morphological heterogeneity of filled rubbers due to a spatially heterogeneous distribution of the filler particles and their agglomeration. The formation of a physical elastomer/filler network can produce another type of heterogeneity, which results from the heterogeneous distribution of adsorption network junctions and imperfections of the network, e.g., chains that are not attached to the carbon black gels and chain loops.

(iii) The elastomer /filler interface, which reveals a strongly hindered chain mobility compared to the bulk rubber.[13,14,28]

2. Heterogeneity of the Network Structure As Studied by T_2 Relaxation. A quantitative analysis of the decay shape is not always straightforward due to the complex origin of the relaxation function itself[28] and the structural heterogeneity of the long chain molecules. Nevertheless, several examples of the detection of structural heterogeneity by T_2 experiments have been published, for example, the analysis of the gel/sol content in cured[29,30] and filled elastomers,[31] the estimation of the fraction of chain-end blocks in linear and network elastomers,[32−34] and the determination of a distribution function for the molecular mass of network chains in cross-linked elastomers.[35,36]

The sensitivity of the T_2 experiments to the molecular scale heterogeneity is due to the local origin of the relaxation process, which is predominantly governed by the near-neighbor environment and intrachain effects for T_2 relaxation at temperatures well above the T_g.[13] Therefore, the submolecules concept can be used to describe the relaxation behavior.[28] In

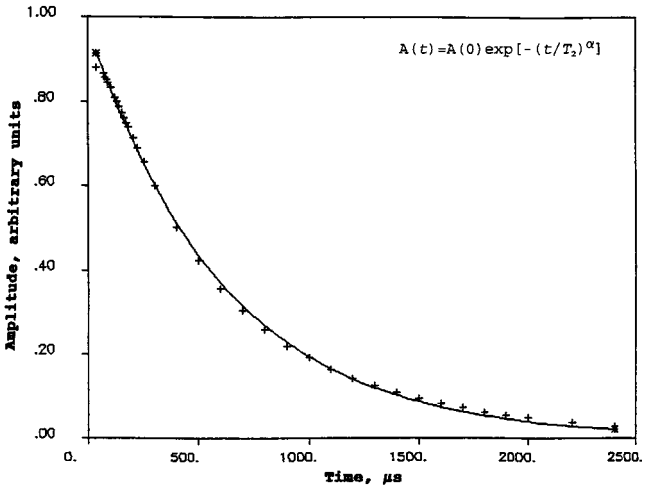

Figure 1. ^{1}H T_2 relaxation decay for unfilled EPDM-2 at 40 °C (points). The line represents the result of a least-squares adjustment of the decay with a Weibull function.

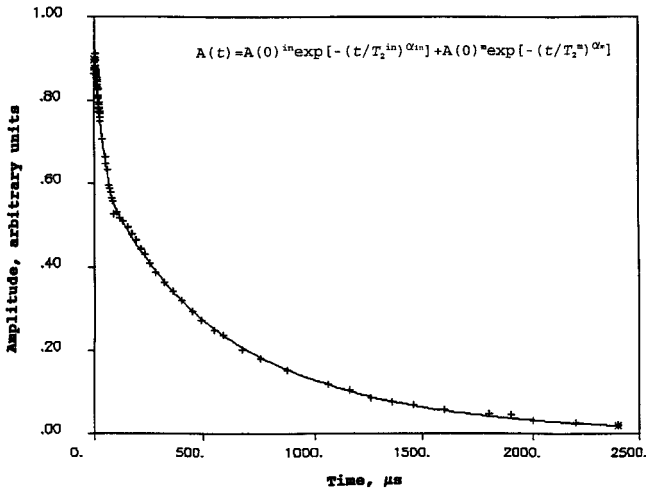

Figure 2. ^{1}H T_2 relaxation decay for bound EPDM rubber (N110/285/boiling *o*-xylene) at 125 °C (points). The line represents the result of a least-squares adjustment of the decay using a two-component model, which is a sum of Weibull functions.

a simplified picture, the total T_2 relaxation decay for a heterogeneous elastomer is a weighted sum of decays from the different submolecules which are defined as the network chains between the chemical and the physical junctions, the chain loops, and the chain-end blocks. Because of differences in the long spatial scale mobility of these submolecules, they possess a different relaxation behavior. The relative contribution of the submolecules to the total decay is proportional to the number of protons that are attached to these chain fragments.

The following two different approaches are used in the present study to describe the T_2 decays in the EPDM matrix. If the transverse magnetization monotonically decays as a function of time, the decay is fitted with a single function. This is usually observed in unfilled EPDM vulcanisates.[20] It suggests a rather uniform chain mobility over the sample volume and/or a strong coupling in chain motions between the discrete domains, which are assumed to result from sample heterogeneity. If the transverse magnetization reveals two distinct components with greatly different mean decay time, the T_2 decays are represented by the sum of the two discrete relaxation components. This suggests a spatial heterogeneity of the chain motion in the rubber matrix, which is caused by the morphological heterogeneity of the samples on a scale of at least 1−10 nm. The relaxation components in this case are assigned to discrete domains in the sample, each exhibiting a unique relaxation behavior independent of its surroundings. The relative intensity of these components represents the fraction of protons in the domains with a different chain mobility.

Results and Discussion

EPDM−Carbon Black Interface. To obtain unambiguous information about the interfacial material in a carbon black filled EPDM, the bound rubber, which contains 285 phr carbon black N110, was taken for the NMR experiment. The fraction of the interfacial EPDM in this sample should be sufficient for an accurate study by the T_2 relaxation experiment because of its high filler content. The ^{1}H T_2 relaxation decay for the unfilled EPDM and the bound rubber is compared in Figures 1 and 2. A good description of the T_2 decay for the unfilled EPDM can be given by a single Weibull function, as shown in Figure 1. As can be seen in Figure 2, the T_2 decay for the bound rubber consists of two distinct components. At the time interval from $t = 0$ to $t \approx 60$ μs, the amplitude of the decay, $A(t)$, decreases fast. At $t > 60$ μs, the decay rate slows down, and the decay amplitude approaches the equilibrium zero value after 2−3 ms. The statistically most relevant fit of the T_2 decay for the bound rubber is obtained for a linear combination of two Weibull functions:

$$A(t) = A(0)^{\mathrm{in}} \exp[-(t/T_2{}^{\mathrm{in}})^{\alpha_{\mathrm{in}}}] + A(0)^{\mathrm{m}} \times \exp[-(t/T_2{}^{\mathrm{m}})^{\alpha_{\mathrm{m}}}] \quad (4)$$

where $A(0)$ is the fractional amplitude of the relaxation components, T_2 is the characteristic decay time, and α is the decay shape parameter that might be related to the distribution of the relaxation time. The superscripts "in" (interface) and "m" (matrix) relate to the fast-decaying and the slowly-decaying components, respectively. The empirical Weibull function is rather often used to describe the relaxation in inhomogeneous materials. The $T_2{}^{\mathrm{in}}$ and $T_2{}^{\mathrm{m}}$ values at 125 °C equal 40 ± 2 and 590 ± 20 μs, respectively. The fraction of the $T_2{}^{\mathrm{in}}$ component in the decay equals 28 ± 3%.

Since the fast-decaying component could originate both from the EPDM and from a small fraction of protons in the carbon black itself, an additional T_2 experiment was performed for pure carbon black N110. The amount of carbon black taken was equal to that in the bound rubber sample. No significant signal was detected. Two other phenomena should also be discussed with respect to the origin of a fast-decaying component: (i) the magnetic field gradients introduced by the filler particles and (ii) the paramagnetic impurities from carbon black itself and free radicals, which could be caused by the milling.[14] In filled rubbers, magnetic susceptibility differences between carbon black and rubber lead to B_0 inhomogeneity at the rubber−filler interface. T_2's of the order of milliseconds are predicted from this field inhomogeneity.[38] These values are significantly longer compared to $T_2{}^{\mathrm{in}}$, which suggests that the field inhomogeneity is of minor importance for the $T_2{}^{\mathrm{in}}$ relaxation. Magic-angle spinning (MAS) techniques allow to average out B_0 inhomogeneity to a large extent. The ^{13}C NMR spectra for bound rubber (N110/285/boiling *o*-xylene), which are recorded at the MAS frequency of 3600 Hz, show that the line widths for the bound rubber are about twice as large as those for pure EPDM, and the ^{13}C chemical shifts of most peaks in the bound rubber have shifted slightly to higher field

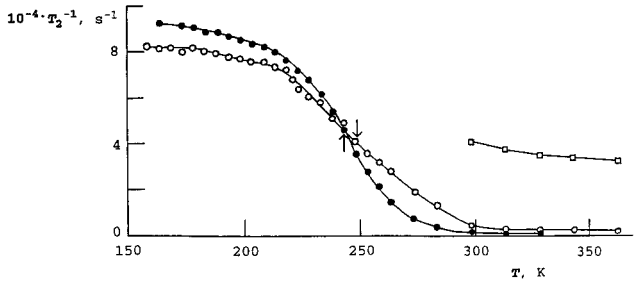

Figure 3. Temperature dependence of the T_2 relaxation rate for unfilled EPDM-2 (●) and the relaxation rate $(T_2^{m})^{-1}$ (○) and $(T_2^{in})^{-1}$ (□) for bound rubber (N110/285/boiling *o*-xylene). Arrows denote the T_g(NMR).

relative to pure EPDM.[39] It is therefore concluded that the T_2^{in} relaxation is not due to the effects of magnetic susceptibility. A previous study of carbon black filled rubbers has shown that the paramagnetic impurities are not the origin of the fast-decaying component.[40] Moreover, the two-component relaxation is observed in the carbon black bound EPDMs which were prepared by 80 days extraction in the presence of a free-radical scavenger, DTPC. In addition, the two-component NMR relaxation behavior is also observed for a silica-filled poly(dimethylsiloxane),[13] which apparently contains less paramagnetic impurities than the carbon black filled elastomers. Thus, the fast-decaying component in the filled EPDM would appear to be caused by the motional constraints for the EPDM chains at the filler particles.

In Figure 3 the temperature dependence of the $(T_2^{m})^{-1}$ is compared to the relaxation rate for unfilled EPDM-2. In the complete temperature range studied, the relaxation rate $(T_2^{m})^{-1}$ for the bound rubber is rather similar to the relaxation rate $(T_2^{u})^{-1}$ in the unfilled EPDM. The T_2^{-1} value is nearly constant below T_g. The glass transition at the time scale of the NMR experiments, i.e., 10−100 μs, causes a sharp decrease in the T_2^{-1} value. The temperature of the NMR glass transition, T_g(NMR), is determined as the temperature at which the relaxation rate has the following value:[37]

$$T_2^{-1} = [(T_2^{rl})^{-1} - (T_2^{ht})^{-1}]/2 \qquad (5)$$

where $(T_2^{rl})^{-1}$ and $(T_2^{ht})^{-1}$ are the relaxation rate at the low- and high-temperature limits of the temperature dependence of the T_2^{-1}, respectively. The average frequency of the local chain motion, ν_c, at the T_g(NMR) equals 1.5×10^4 s^{-1}, according to the relationship $\nu_c \approx (2\pi T_2^{rl})^{-1}$.[37] It is noted that T_g(NMR) for polymers is comparable with the glass temperature as measured by the dynamic mechanical experiment at a frequency of about 10 kHz.

As far as the other relaxation component in the bound rubber is concerned, its value, $(T_2^{in})^{-1}$, does not depend on temperature and is comparable to the value of $(T_2^{u})^{-1}$ for the unfilled EPDM in the glass transition range, even at 150 °C.

The above results provide considerable evidence for a strong dynamic heterogeneity in the bound rubber at temperatures above T_g(NMR). *First*, the two-component decay indicates the molecular scale heterogeneity of the EPDM chains in the bound rubber. These relaxation components are assigned to different EPDM microregions in the bound rubber, since the T_2 relaxation is mainly determined by chain motion in a near-neighbor environment. *Second*, the chain mobility in these two microregions is strongly different in a wide temperature

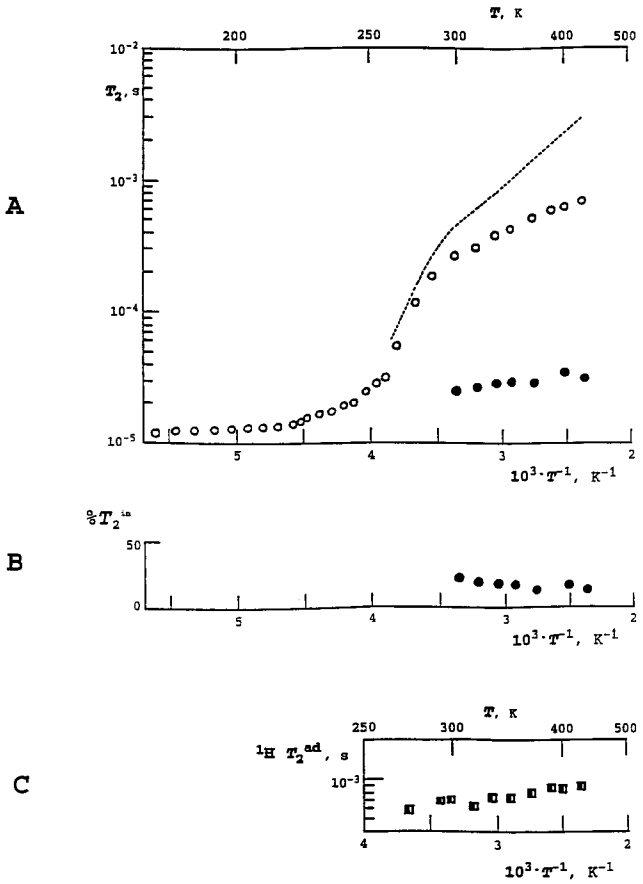

Figure 4. Temperature dependence of the relaxation time T_2^{in} (●) and T_2^{m} (○) for bound rubber (N110/285/boiling *o*-xylene) (A). The dotted line shows the temperature dependence of the T_2^{u} for unfilled EPDM-2. The temperature dependence of the fraction of T_2^{in} (B). The temperature dependence of the relaxation time T_2^{ad} (C).

range, as shown in Figure 3. In this respect it should be noted that the larger the $(T_2)^{-1}$ value, the less mobile the chain segments are. The chain mobility in one microregion of the bound rubber is similar to that in the unfilled EPDM. In contrast, the chain mobility for the other microregion is strongly hindered in the temperature range of this study. Moreover, the chain mobility in this microregion is almost independent of temperature and is comparable with that for the unfilled EPDM in the T_g range. It is therefore concluded that one microregion in the bound rubber originates from an *EPDM/carbon black interface* covering the surface of the carbon black, and the other one consists of *the elastomer matrix* outside of this interface. Since the statistical segment of EPDM chains is about three monomer units, the rotational and translational chain mobility increases fast as the distance from the adsorption layer increases.

The strongly hindered chain mobility in the interface is apparently caused by physical adsorption of the EPDM chain units to the surface of the carbon black particles. Moreover, a loss of configurational entropy of the polymer chains near the filler surface could also contribute to the restriction of the chain mobility in the interface.[13]

T_2^{in} at 20 °C is about twice as large as T_2 in the glassy state, as shown in Figure 4A. This means that, despite the strong physical adsorption, the chain units at the interface are not rigidly fixed to the surface of the carbon black. Upon an increase in the temperature from 20 to

150 °C, the fraction of the EPDM chain units in the interface decreases slightly (Figure 4B), whereas the T_2^{in} value increases from 26 to 40 μs because of an increase in the chain mobility in the interface. It is thought that these changes can arise from a shift of the overall adsorption−desorption equilibrium to chain desorption from the weakest adsorption sites at the surface of the carbon black,[13] because of the heterogeneity of the surface energy of the carbon blacks.[8]

The T_2^{in} value could provide qualitative information regarding the rigidity of the interface in carbon black filled EPDM. Numerous NMR studies for pure polymers and blends show that the temperature dependence of $(T_2)^{-1}$ is qualitatively similar to that of the mechanical modulus as measured at about 1−10 kHz.[37,41] The higher the $(T_2)^{-1}$ value, the more rigid the material. At temperatures from 20 to 150 °C, the $(T_2^{in})^{-1}$ value is in the range of the (T_2^{-1}) value for the unfilled EPDM at T_g(NMR). It is therefore assumed that the EPDM/carbon black interface is semirigid in the complete temperature range studied.

The local chain motion outside of the interface is not very different from that in the unfilled EPDM, since the T_g(NMR) for the matrix EPDM in the bound rubber is only a few degrees centigrade higher than that for the unfilled EPDM, as can be seen in Figure 3. It appears that the local chain mobility increases fast when moving away from the interface because of a well-shaped two-component decay for the bound rubber and because of the large difference in the T_2^{in} and T_2^{m} values. The "steplike" change of the local chain motions with increasing distance from the interface is caused by two reasons: (1) the local origin of the surface field force of the carbon black and (2) the high flexibility of the EPDM chain.

The thickness of the EPDM/carbon black interface in the bound rubber is estimated from the value obtained for the fraction of chain units in the interfacial layer, the specific surface, and volume fraction of the carbon black. The thickness of the interfacial layer is about 0.7 nm if it is assumed that the entire carbon black surface is covered by a uniform EPDM layer of a constant thickness. This value should be increased by a factor of ≈1.5−2 if a significant part of the carbon black surface is not accessible to the EPDM chains due to an agglomeration of carbon black aggregates. Thus, the thickness of the interfacial layer is slightly above the effective diameter of ethylene and propylene chain units, which is about 0.48 and 0.66 nm,[42] respectively. It can therefore be concluded that the direct energetic effect of the carbon black surface force field can be estimated to be of the order of one to two monolayers. A simplified graphic representation of the EPDM chains at the surface of the carbon black is shown in Figure 5.

The Mean Molar Mass of the EPDM Chains Between the Adjacent Adsorption Junctions along a Chain. The filler particles that are covered by the semirigid interface can be considered as multifunctional physical cross-links, as shown in Figure 6. Pseudosolid spin echo experiment proves that, even in the presence of solvent, translational chain mobility in silica and carbon black filled rubbers is hindered due to constraints from filler particles.[42,43] Because of the large total interfacial area in filled elastomers, the density of these physical network junctions is apparently large.

The value of T_2^{m} at temperatures above 90 °C can be used for a quantitative analysis of the mean molar mass

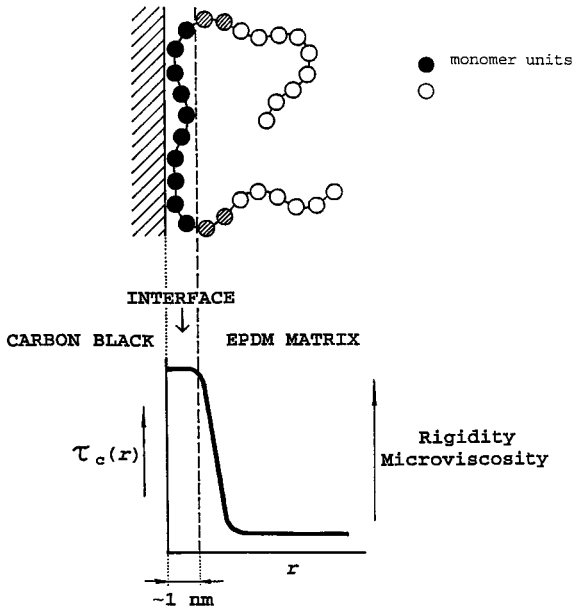

Figure 5. A simplified graphic representation of EPDM chains at the carbon black surface. Low mobile monomer units in the interface and mobile chain units outside of the interface are shown by solid and open points, respectively. The rotational and translational mobility of a few chain units next to the adsorption layer along the chain (dashed points) is somewhat hindered compared to those in the matrix. The low mobile chain fragments in the interface provide adsorption network junctions for the rubber matrix. At the bottom, the spatial profile of the correlation time τ_c of the chain motion is shown schematically as a function of distance, r, from the carbon black surface. The τ_c is the "average" time for a single reorientation of a chain unit.

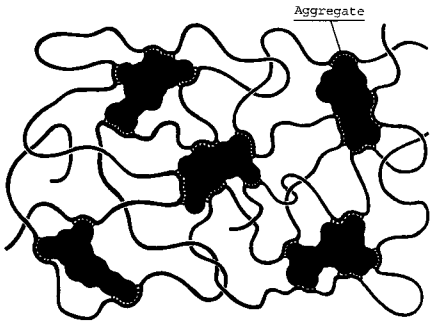

Figure 6. A schematic drawing of the physical network structure in a carbon black filled elastomer. Elastomer−carbon black adsorption junctions are indicated by the sign • • •. The length scales in this figure as well as the volume ratio EPDM/carbon black are not sustained. For simplicity, none of the contacting carbon black aggregates, which form agglomerates, are shown.

of the chemical and the physical network chains in an EPDM rubber.[20] In Figure 4A the temperature dependence of the T_2 relaxation time for unfilled EPDM, T_2^{u}, is compared with that for the rubber matrix in bound rubber, T_2^{m}. Both relaxation times are similar in the glass transition range. A significant difference in the T_2^{u} and T_2^{m} values is observed at temperatures well above T_g(NMR). At these temperatures, the T_2 relaxation is mainly determined by large-scale chain motions.[15,28] A continuous increase in the T_2^{u} value is attributed to the increase of the spatial scale and frequency of the chain motions in unfilled EPDM. The T_2^{m} value for bound rubber is significantly smaller than T_2^{u} for unfilled EPDM. This means that carbon black significantly restricts the long spatial scale mobility of

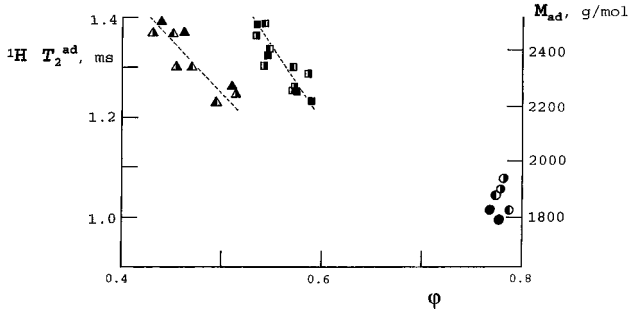

Figure 7. T_2^{ad} and M_{ad} as a function of the volume fraction of carbon blacks in bound rubber. The type of carbon black is indicated by circles, squares, and triangles for N550, N330, and N110, respectively. Solvents used for the extraction are indicated by solid symbols for *n*-hexane, by left-side-closed symbols for a mixture of *o*-xylene with 2 wt % of acetonitrile, and by right-side-closed symbols for *n*-hexane in an ammonia atmosphere. The dashed lines are a guide to the eye. The average molar mass between adsorption network junctions from EPDM/carbon black interface is shown on the vertical axis on the right.

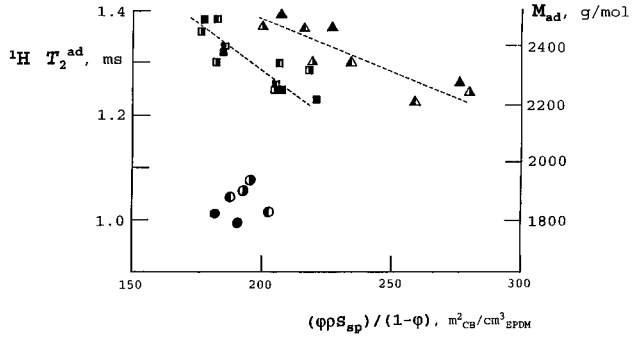

Figure 8. T_2^{ad} and M_{ad} as a function of the maximum possible EPDM−carbon black contact area per unit volume of the elastomer, $\Psi = \varphi\rho S_{sp}/(1 - \varphi)$, in bound rubber. The symbols of this figure correspond to the ones of Figure 7. The dashed lines are a guide to the eye. The average molar mass between adsorption network junctions from the EPDM/carbon black interface is shown on the vertical axis on the right.

EPDM chains outside of the interface compared with the unfilled sample. It is suggested that these restrictions originate from adsorption network junctions at the interface, since the fraction of chemical cross-links that could arise during the milling is rather low, as will be shown below. In a greatly simplified picture, the overall relaxation rate $(T_2^m)^{-1}$ can be expressed as the weighted mean of the relaxation rate $(T_2^u)^{-1}$ with the $(T_2^{ad})^{-1}$ value, which is related to the effect of the adsorption network junctions on long spatial scale chain motion:

$$(T_2^{\,m})^{-1} = (T_2^{\,u})^{-1} + (T_2^{\,ad})^{-1} \qquad (6)$$

It should be noted that the effect of chain entanglements and chain loops on the relaxation is accounted for by the $(T_2^u)^{-1}$ value. Figure 4C shows that the $(T_2^{ad})^{-1}$ value does not increase with increasing temperature, contrary to the observation for unfilled EPDM. Such a high-temperature plateau of the T_2 relaxation is also observed for unfilled networks.[15,20,28] A value of T_2 at the plateau is determined by chemical cross-links as well as by temporary and trapped chain entanglements in unfilled EPDM.[20] We suggest here that the T_2^{ad} value at the high-temperature plateau can be related to the average molar mass of EPDM chains between adsorption junctions in the same way as with the vulcanisates.

The T_2^{ad} value at 125 °C is used for the calculation of the molar mass of network chains in bound rubber, M_{ad}, as described previously.[20] The shorter T_2^{ad}, the smaller the M_{ad} value becomes. The Gaussian chain statistic is suggested for this calculation. It should be noted that the Gaussian characteristics of the elastomeric chains can be disturbed by the nonpenetrable filler particles placed in the elastomer matrix, as was recently shown by Monte Carlo simulations.[45] However, according to another author,[46] elastomer chains in a filled network are still Gaussian, as in a pure melt. Because of this uncertainty, the calculated M_{ad} should be considered as an estimate of the absolute value.

Figure 7 shows the T_2^{ad} and M_{ad} values as functions of the volume fraction of carbon black in bound rubbers, φ. M_{ad} is tentatively related to bridging chains between neighboring carbon black particles and aggregates. For bound rubbers that are filled by the same type of carbon black, the M_{ad} value decreases as the carbon black content increases. At $\varphi \approx 0.55$, M_{ad} is smaller for the samples filled with N110 compared to the ones filled with N330. It is therefore concluded that the density of the adsorption junctions in the rubber matrix increases with increasing carbon black surface area and with increasing filler content. The effect of carbon black agglomeration on M_{ad} can be revealed using the plot of T_2^{ad} and M_{ad} against the maximum possible EPDM/filler contact area per unit volume of the elastomer, $\Psi = \varphi\rho S_{sp}/(1 - \varphi)$, which is shown in Figure 8. If the entire surface of carbon black were available for the adsorption of EPDM chains and if the surface structure were the same, one would expect the same T_2^{ad} value for samples with the same value of Ψ, regardless of the type of carbon black. However, this is not observed in the bound rubbers studied. The smaller the specific surface of carbon black, the shorter the T_2^{ad} value becomes. This means that the fraction of carbon black surface that is occupied by EPDM decreases with increasing specific surface of the carbon black. This can be caused by agglomeration of carbon black aggregates. Thus, analysis of the T_2^{ad} value could provide information on the agglomeration of carbon black in the filled samples.

The calculated value of M_{ad} is in the range of from 1800 to 2500 g/mol and depends on the type and the content of carbon blacks in bound rubbers, as shown in Figures 7 and 8. The values are comparable with the molar mass of network chains in unfilled EPDM vulcanisates.[20]

According to the theory proposed for bound rubber,[47] the bound rubber should mainly contain a high molar mass fraction of elastomer chains. A single EPDM chain in bound rubber has about 50−70 adsorption junctions at the surface of the carbon black according to M_{ad} and M_w values. It appears that the probability of a simultaneous desorption of each EPDM chain from all active sites on the surface of carbon black during extraction is rather low. This conclusion is supported by the result of the extraction experiment, which reveals that the content of bound rubber does not depend on the quality of the solvent used (see Table 4). It is concluded that adsorption junctions form a quasi-permanent physical network in bound rubbers.

Mean Distance Between Adsorption Junctions in Relation to Mean Thickness of EPDM Layer Covering the Surface of Carbon Black in Bound Rubber. Some information about the structure of the physical network in bound rubbers can be provided by analysis of the mean distance between the adjacent

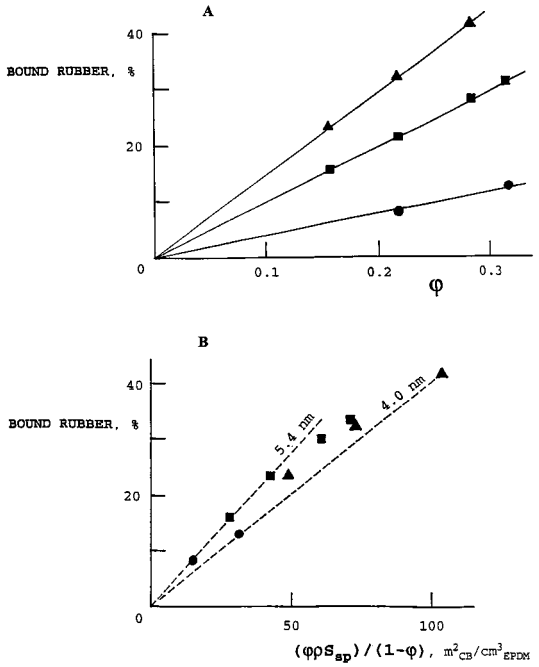

Figure 9. Content of bound rubber as a function of the volume fraction of carbon black, φ, (A) and the maximum possible EPDM−filler contact area per unit volume of the rubber, $\varphi\rho S_{sp}/(1-\varphi)$ (B) in compounds. The symbols used in this figure correspond to the ones of Figure 7. The solid lines in (A) are a guide to the eye. The dashed lines in (B) were calculated using the Pliskin-Tokita equation (eq 7) for $f = 1$.

adsorption junctions along a chain, $\langle R_{ad}^2\rangle^{0.5}$, with respect to the thickness of the bound layer, R_0. These values are estimated below.

To estimate the mean thickness of the bound layer, the content of the bound rubber, R_b, is studied as a function of φ and $\Psi = \varphi\rho S_{sp}/(1-\varphi)$ for the compounds. The linear relationship of R_b with φ is observed for bound rubbers that are filled with the same type of carbon black (see Figure 9A). The increase in the specific surface area of the carbon black causes an increase in the R_b value. Furthermore, it can be observed that the line which represents the relationship between R_b and φ goes through the origin. This implies that the bound rubber is formed mainly due to the interactions between EPDM and carbon black and that the fraction of the chemical cross-links in the rubber itself, which could arise during milling, is apparently low.

The dependence of R_b on the maximum possible EPDM/filler contact area per unit volume of the elastomer is shown in Figure 9B. The mean thickness of the bound layer is estimated from this plot using the Pliskin−Tokita equation.[11] This equation is derived for a rather idealized model. The model assumes that a carbon black surface is covered by a uniform bound layer, which results in the equation

$$R_b = R_0 f\,[\varphi\rho S_{sp}/(1-\varphi)] + G \qquad (7)$$

where R_0 is the mean thickness of the bound layer, which is the sum of the elastomer/filler interface, and of the rubber matrix outside of the interface; G is the fraction of gel in the unfilled rubber (G equals zero for the samples studied); f is the fraction of the total surface area of carbon black, which is exposed to EPDM. The f value for the bound rubbers studied is the missing parameter due to unknown agglomeration of the carbon black on a spatial scale below micrometers. For $f = 1$, the R_0 value represents the lowest possible thickness of the bound layer. It can be seen in Figure 9B that R_b increases almost proportionally to the increase in Ψ value, regardless of the type of carbon black. Some deviation from linearity is attributed to the effect of the agglomeration of the carbon black, which reduces the EPDM/carbon black contact area, as was already concluded from the T_2^{ad} analysis. The two extreme slopes for the data points provide the range of R_0 values. Under the above assumption, the mean thickness of the bound layer equals 4.0−5.4 nm.

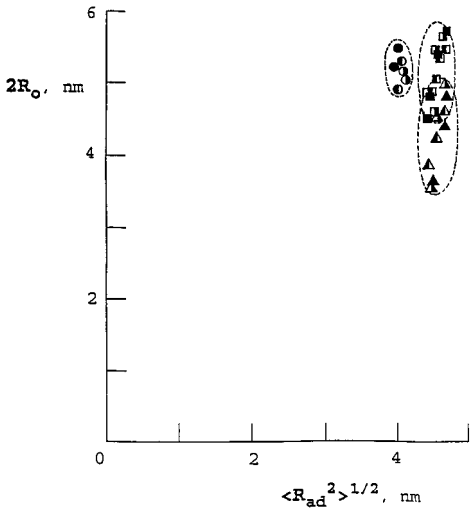

Figure 10. Double thickness of the bound layer, $2R_0$, versus the mean distance between adjacent adsorption junctions along a chain. The symbols used in this figure correspond to the ones of Figure 7.

The mean distance between the adjacent adsorption junctions along a chain, $\langle R_{ad}^2\rangle^{0.5}$, is estimated from the M_{ad} value, suggesting Gaussian chain statistics:

$$\langle R_{ad}^2\rangle = nN_{ad}C_\infty l_0^2 \qquad (8)$$

where n is the average number of backbone bonds per monomer unit, N_{ad} is the number of monomer units between adjacent adsorption junctions along a chain, C_∞ is the number of backbone bonds in the statistical segment, and l_0 is the average main-chain bond length. The C_∞ of 6.62 for alternating ethylene propylene copolymer is used for the $\langle R_{ad}^2\rangle^{0.5}$ calculation.[48]

In Figure 10 the $\langle R_{ad}^2\rangle^{0.5}$ value is compared with the average thickness of the bound layer $2R_0$. Because of the crude approximations made for the calculation of these two values, no elaborate analysis is possible. However, qualitative information about the network structure in the bound rubbers studied can be obtained. It can be seen that the $\langle R_{ad}^2\rangle^{0.5}$ value is comparable with the $2R_0$ value for all the samples studied. This suggests that the physical network in bound rubbers is largely formed by bridging chains between the neighboring carbon black aggregates. As observed in Figure 10, the data points for the bound rubbers studied are located in three slightly different areas. This could be due to the following causes. First, the effect of agglomeration of carbon black is neglected for the calculation of R_0. Moreover, the physical network structure in the samples studied could be somewhat different due to differences in surface activity and irregularity of the aggregates surface for the carbon blacks used.

Because of the large fraction of bridging network chains in bound rubber, it can be assumed that a

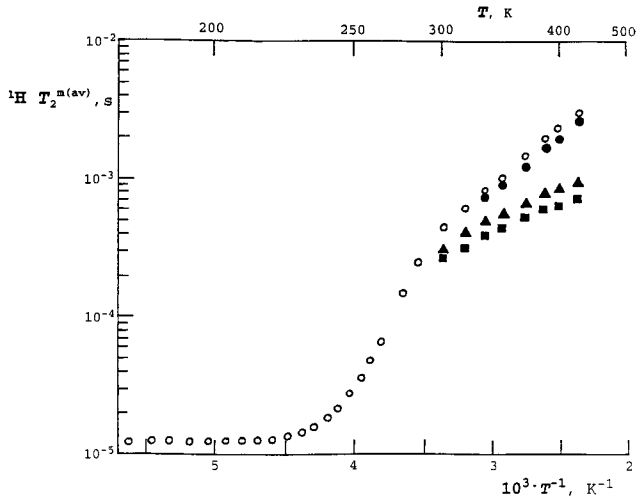

Figure 11. Temperature dependence of the relaxation time T_2 for unfilled EPDM-2, T_2^u, (open circles), and for the elastomer matrix outside of the EPDM/carbon black interface, $T_2^{m(av)}$, in the following samples: compound N110/85.5 (solid circles), bound rubber N110/210/(X/AN) (triangles), and N110/285/boiling *o*-xylene (squares). A Weibull function and a normal distribution of exponents are used for a least-squares adjustment of the T_2 decays at temperatures below and above 250 K, respectively. Because the T_2 values for unfilled and filled samples are similar below room temperature, the $T_2^{m(av)}$ value for all samples is shown only at temperatures above 300 K.

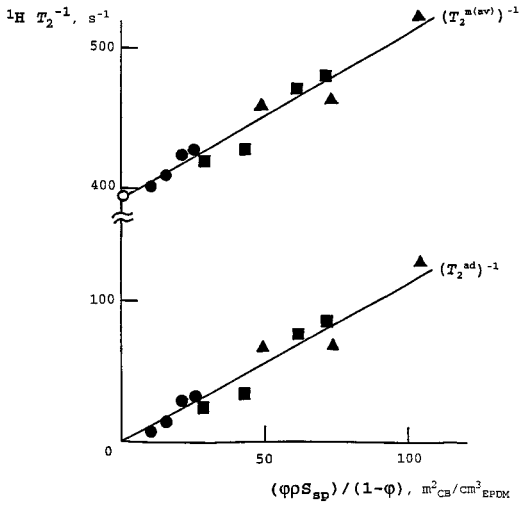

Figure 12. Relaxation rate $(T_2^{m(av)})^{-1}$ and $(T_2^{ad})^{-1}$ at 125 °C as a function of the maximum possible EPDM−carbon black contact area, $\Psi = \varphi\rho S_{sp}/(1 - \varphi)$, in compounds. The symbols used in this figure correspond to the ones of Figure 7.

continuous EPDM/carbon black physical network is formed in bound rubber. The carbon black aggregates act as multifunctional physical cross-links in this network. It is therefore highly probable that the adsorption network junctions arising from the EPDM/carbon black interface are of great importance for the viscoelastic behavior of these materials.

Heterogeneity of Physical Network Structure in Carbon Black Filled Compounds. In contrast with the bound rubber, T_2 decay both for initial EPDM and the rubber matrix in compounds has a rather complex shape, which undergoes significant changes with increasing temperature above −25 °C. One-component models do not provide a statistically relevant fit of these T_2 decays. Therefore, a normal distribution of exponential functions with the mean $T_2^{m(av)}$ value is used to describe the T_2 decay in the whole temperature range studied. In Figure 11 the temperature dependence of $T_2^{m(av)}$ for a few filled EPDMs is compared with T_2 relaxation time, T_2^u, for the corresponding unfilled EPDM. It can be seen that the $T_2^{m(av)}$ value in filled samples decreases as the carbon black content in the samples increases.

To reveal the effect of carbon black on the T_2 relaxation rate in the rubber matrix, the $(T_2^{m(av)})^{-1}$ value at 125 °C is analyzed as a function of Ψ. The relaxation rate $(T_2^{m(av)})^{-1}$ and T_2^{ad} increases with increasing Ψ value, regardless of the type of carbon black, as shown in Figure 12. Consequently, the mean density of the adsorption junctions in the rubber matrix increases with increasing EPDM/carbon black contact area per unit volume of the rubber. Since the relaxation rate $(T_2^{m(av)})^{-1}$ represents the mean value for the rubber matrix, both a random and a heterogeneous distribution of adsorption network junctions in the rubber matrix can cause the observed change in the relaxation rate. Two extreme cases are considered below to explain the dependence of the $(T_2^{m(av)})^{-1}$ on Ψ, i.e., (i) the random distribution of adsorption junctions in the rubber matrix and (ii) a spatially heterogeneous distribution or "bimodal"-like distribution of the adsorption junctions in the rubber matrix. It appears that a heterogeneous distribution of adsorption junctions is more realistic than a homogeneous one, because of the heterogeneous morphology of carbon black filled rubbers.[1]

A highly simplified approach is used to describe the T_2 relaxation. It is assumed that two domains with strongly different densities of the adsorption junctions are present in the rubber matrix. Chain fragments and/or chains in one domain have numerous adsorption contacts with the surface of carbon blacks, whereas chains in the other domain do not interact with the filler surface. The values of $(T_2^{m(un)})^{-1}$ and $(T_2^{m(lo)})^{-1}$ represent the relaxation rate in these areas, where the superscripts "un" (unbound or extractable) and "lo" (loosely bound) relate to the areas with a low and a high density of adsorption network junctions, respectively. The following equation could be used to relate $(T_2^{m(av)})^{-1}$ to the fraction of EPDM chains in "loosely bound" areas in the compounds, R_b^{NMR},

$$(T_2^{m(av)})^{-1} = (1 - R_b^{NMR})(T_2^{m(un)})^{-1} + R_b^{NMR}(T_2^{m(lo)})^{-1} \quad (9)$$

It is assumed that the relaxation rate $(T_2^{m(un)})^{-1}$ is equal to the T_2^u value for unfilled EPDM. It is also suggested that the density of adsorption junctions is the same for the bound rubber and for "loosely bound" areas in the compounds, i.e., $T_2^{m(lo)} \approx T_2^m$, where T_2^m is the T_2 relaxation time for the bound rubber. It is furthermore assumed that the $(T_2^{m(un)})^{-1}$ and $(T_2^{m(lo)})^{-1}$ values do not depend on the carbon black content. This equation does not make any distinction between a possible difference in the spatial scale of the network heterogeneity.

In Figure 13 the calculated value of R_b^{NMR} is shown as a function of the maximum possible EPDM−carbon black contact area per unit volume of the elastomer, Ψ. The fraction of EPDM chains in "loosely bound" domains increases with increasing Ψ, regardless of the type of carbon black. The R_b^{NMR} value is rather close to the content of bound rubber (R_b), as determined by extraction, in the entire Ψ range studied, as can be seen in Figure 13. It should also be mentioned that the $(T_2^{m(av)})^{-1}$

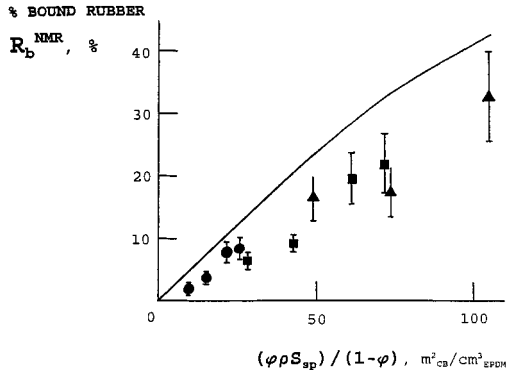

Figure 13. A value of R_b^{NMR} as a function of the maximum possible EPDM−carbon black contact area. The error bars indicate the range of R_b^{NMR} values corresponding to the $T_2^{m(lo)}$ values of 1.3 and 1.12 ms used for R_b^{NMR} calculation. These $T_2^{m(lo)}$ values cover the range of T_2^m in the rubber matrix of bound EPDMs. The solid line represents the content of bound rubber determined by extraction. The symbols used in this figure correspond to the ones of Figure 7.

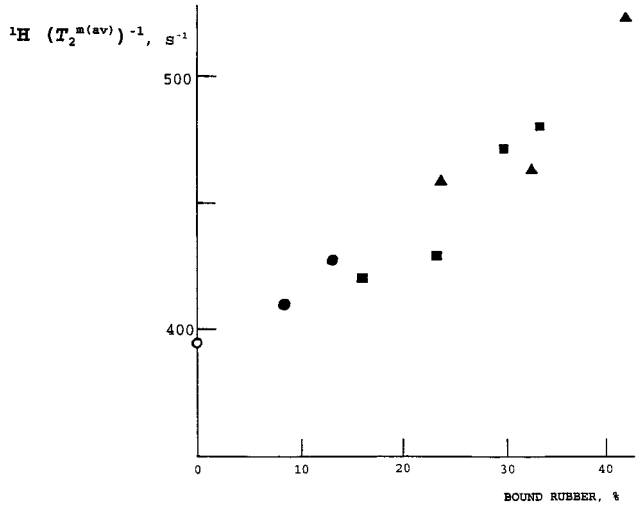

Figure 14. The $(T_2^{m(av)})^{-1}$ value at 125 °C versus the content of bound rubber. The symbols used in this figure correspond to the ones of Figure 7. The open circle shows the $(T_2^u)^{-1}$ value for unfilled EPDM.

value increases proportionally to the increase of the bound rubber content, as shown in Figure 14. Thus, the heterogeneous model for the structure of the physical network in filled EPDM is supported by the correlation which is observed between R_b^{NMR} and $(T_2^{m(av)})^{-1}$ values on one hand and the content of bound rubber on the other hand, as shown in Figures 13 and 14. However, the T_2 experiments for bulk samples are not conclusive for the above models.

The analysis of the heterogeneous distribution of adsorption junctions in compounds is hidden because of the high entanglement density in EPDM which is comparable to the density of adsorption junctions. At the time scale of the NMR experiment, which is in the order of milliseconds, the chain entanglements restrict the long spatial scale dynamics in the same way as chemical and adsorption junctions do.[20]

It is known that the effect of transient chain entanglements on the chain dynamics decreases as the volume fraction of a solvent in swollen gels increases.[49] It could be expected that local swelling in "loosely bound" and "unbound" areas in compounds is different, because of the suggested heterogeneity of the physical network

Table 5. T_2 Values and the Relative Intensity of the Relaxation Component, Which Is Characterized by the $(T_2M^{(lo)})^{sw}$ Value, for Swollen Compound N110/85.5 at 40 °C[a]

fitting model	$(T_2^{m(lo)})^{sw}$, ms	$(T_2^{m(un)})^{sw}$, ms	% $(T_2^{m(lo)})^{sw}$
Exp+exp	1.9 ± 0.1	15.1 ± 0.5	28 ± 2
We+exp	2.2 ± 0.2	16.5 ± 0.7	32 ± 5
CA+exp	1.7 ± 0.1	13.8 ± 0.3	24 ± 3
CA+CA	2.0 ± 0.1	17.5 ± 0.5	37 ± 3

[a] The volume fraction of EPDM in the swollen matrix, V_p, is equal to 0.39. A linear combination of functions is used for least-squares adjustments of the T_2 decay, as follows: two exponential functions (exp+exp), a Weibull and exponential functions (We+exp), two Cohen-Addad functions (CA+CA), and exponential and the Cohen-Addad functions (exp+CA).

structure and spatial effects of the filler in areas with high and low concentrations of carbon black. Therefore, spatial heterogeneity of adsorption junctions in compounds could possibly be evaluated by means of the analysis of the T_2 decays for the swollen samples. To check this assumption, T_2 relaxation experiments have been carried out for swollen compound N110/85.5 as a function of the volume fraction of EPDM in the swollen matrix, V_p.

The T_2 decay for the swollen compound N110/85.5 has a complex shape, which cannot be described by a distribution of exponents. The statistically most relevant description of the T_2 decay for the swollen sample is obtained with two-component relaxation functions. The decay time of these components, $(T_2^{m(lo)})^{sw}$ and $(T_2^{m(un)})^{sw}$, characterizes fast-decaying and slowly-decaying components, respectively. The least-squares adjusted parameters for different optional decay functions are given in Table 5. It can be seen that the fitting functions used provide rather similar values for the relaxation parameters. A linear combination of the Cohen-Addad and exponential functions is used below for the analysis of the T_2 decays in the swollen compound, because these functions have the physical background, which is relevant to the T_2 relaxation in the swollen compound. The Cohen-Addad function well describes the complex shape of the T_2 decays for cross-linked elastomers.[24] An exponential function is often used to describe T_2 decays for oligomer molecules,[28,50] dilute solutions of polymers,[51] and mobile chain-end blocks in elastomers.[32−34]

Figure 15 shows the change in the relaxation times $(T_2^{m(lo)})^{sw}$ and $(T_2^{m(un)})^{sw}$ as a function of decreasing volume fraction of EPDM chains in the swollen matrix, V_p. At $V_p \geq 0.6$, both relaxation times increase as the V_p value decreases. This increase can be due to the following reasons: (1) chain disentanglements; (2) an increase in chain mobility due to a dilution effect and a slight decrease in the density of adsorption junctions due to a detachment of EPDM chains from the weakest adsorption sites at the surface of carbon black. At $V_p \leq 0.6$, the relaxation times $(T_2^{m(lo)})^{sw}$ and $(T_2^{m(un)})^{sw}$ vary as a function of V_p in a different way, as can be seen in Figure 15. The relaxation time $(T_2^{m(un)})^{sw}$ increases continuously as a function of decreasing V_p value. This type of T_2 dependence on V_p is usually observed for polymer solutions.[51,52] In contrast with this, $(T_2^{m(lo)})^{sw}$ reaches its maximum value at $V_p \approx 0.4$ and slightly decreases at lower V_p values. A maximum of the T_2 dependence on V_p is observed in cross-linked polymers.[20,53] The decrease in T_2 at higher solvent contents is thought to reflect the increase in the intrachain proton dipole−dipole interactions as a result of the

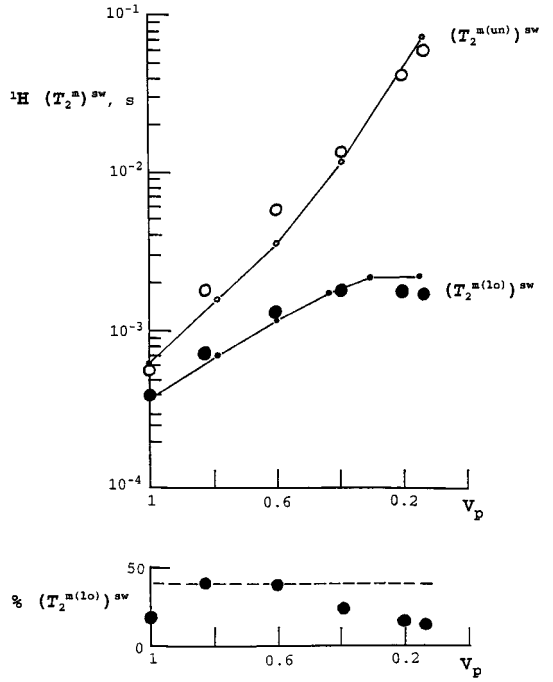

Figure 15. The $(T_2)^{sw}$ relaxation times at 40 °C as a function of the volume fraction of the rubber, V_p, in C_2Cl_4. The T_2 values for unfilled EPDM and bound rubber N110/227/HE are shown by small open and solid circles, respectively. The solid lines which connect these points are a guide to the eye. The large open and solid points show the $(T_2^{m(lo)})^{sw}$ and $(T_2^{m(un)})^{sw}$ values for compound N110/85.5, respectively. The relative fraction of the $(T_2^{m(lo)})^{sw}$ relaxation component is shown at the bottom. The T_2 decays for unfilled EPDM, the bound rubber, and the compound were least-squares adjusted using an exponential function, the Cohen-Addad function, and a linear combination of an exponential and the Cohen-Addad functions, respectively.

network chain elongation upon a progressive increase in the solvent fraction in swollen gel, which results in more efficient T_2 relaxation.[28,53] In the compound, the moderate change of the $(T_2^{m(lo)})^{sw}$ value at $V_p \leq 0.6$ could be caused (i) by chain slippage and/or chain detachments from the carbon black surface and (ii) by spatial effects of the filler aggregates, which can restrict local swelling inside carbon black agglomerates.

In Figure 15 the relaxation times $(T_2^{m(lo)})^{sw}$ and $(T_2^{m(un)})^{sw}$ of the compound are compared with the T_2 value for swollen samples of unfilled EPDM and bound rubber N110/225. The $(T_2^{m(un)})^{sw}$ value is very close to the T_2 value for swollen, unfilled EPDM. It can therefore be concluded that this relaxation component in the swollen, filled sample arises from EPDM chains and/or chain fragments with a limited number of adsorption junctions. The relaxation time $(T_2^{m(lo)})^{sw}$ is similar to the T_2 value for the rubber matrix in swollen, carbon black bound rubber. Therefore, this relaxation component apparently originates from EPDM chains with numerous elastomer−carbon black interactions, similar to that in the bound EPDM. The relative fraction of the $(T_2^{m(lo)})^{sw}$ relaxation component, percent $(T_2^{m(lo)})^{sw}$, is comparable to the fraction of bound EPDM in the compound. It appears that swelling does not cause significant changes in the heterogeneous morphology of the compound. This suggests that the formation of the bound rubber is caused by multiple adsorption of one fraction of the elastomer to the carbon black surface. This adsorbed EPDM forms a quasi-permanent elastomer/carbon black network. The other fraction of the elastomer has a relatively low number of adsorption

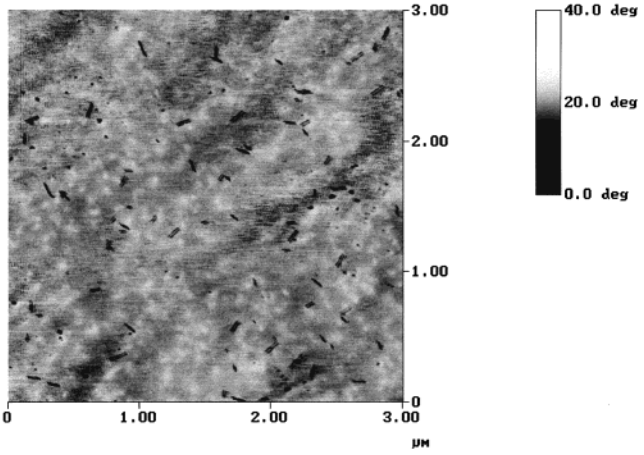

Figure 16. Force modulation AFM image for EPDM−carbon black compound filled with carbon black N110.

network junctions or no junctions at all.

The T_2 experiments for the swollen sample provide strong evidence of a "bimodal" structure of the physical network in filled EPDM. This result is supported by the atomic force (AFM) and the scanning tunneling (STM) micrgraphs. All three AFM modes, i.e., topography, force, and force modulation, and SFM images reveal a heterogeneous structure of the samples. A particularly high contrast was achieved using force modulation. A typical AFM force modulation image is shown in Figure 16. Usually, the surface structure consists of small carbon black grains of about 50 nm in diameter (black areas). In addition, a few bigger carbon black agglomerates are observed whose size varies in the range 500−1500 nm. It appears that the microhardness of the EPDM matrix varies through the sample surface. This is apparently caused by a difference in density of physical EPDM−carbon black junctions.

It can be concluded that *one fraction of EPDM* has multiple adsorption interactions with the carbon black surface, similar to the situation in the bound rubber. These network chains are characterized by the relaxation time $(T_2^{m(lo)})^{sw}$. According to the terminology used, these chains are called *loosely bound EPDM*, as opposed to *a tightly adsorbed layer or elastomer/carbon black interface*.[14,54] The fraction of tightly bound rubber in compounds is a few percent. *The other fraction of EPDM*, which is characterized by the relaxation time $(T_2^{m(lo)})^{sw}$, corresponds to *unbound or extractable rubber*. Apparently, this heterogeneity is caused by carbon black agglomeration. Carbon black aggregates are not randomly distributed in the elastomer matrix because of the difference between elastomer/carbon black and carbon black/carbon black interactions, which is thought to be the intrinsic origin of agglomeration of carbon blacks. Referring to the long-standing dilemma "is bound rubber indicative or operative?",[12] we can conclude that a three-dimensional, heterogeneous elastomer−carbon black network actually exists in filled EPDM.

For compounds filled with carbon black N110 and N330, the network heterogeneity is mainly caused by the effect of agglomeration, since the mean distance between carbon black aggregates is significantly lower than the chain dimension, $\langle R_0^2 \rangle^{0.5}$, for EPDM chains, as can be seen in Figure 17. The bimodal network structure in EPDM/N550 compounds apparently results from carbon black agglomeration and from the rather large distance between the carbon black particles.

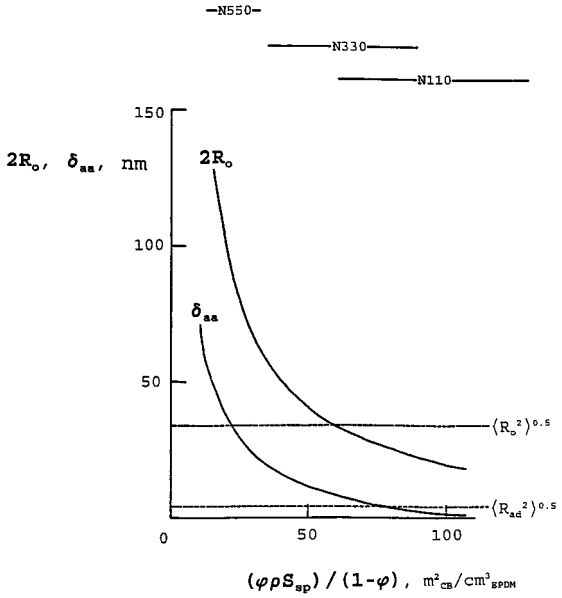

Figure 17. Twice the average thickness of the EPDM layer at the carbon black surface, $2R_0$, and the mean distance between carbon black agglomerates as a function of the maximum possible EPDM−carbon black contact area. The dashed lines show the mean distance between adjacent adsorption junctions along a chain, $\langle R_{ad}^2\rangle^{0.5}$, and the mean end-to-end distance, $\langle R_0^2\rangle^{0.5}$, for EPDM chains. The range of Ψ values for the compounds filled with different types of carbon black is shown by horizontal bars.

Table 6. T_2 Relaxation Time for Unfilled an Filled EPDM Compounds (A) and the Vulcanisates (B)

content of N550, phr	(A) T_2, ms	(B) T_2, ms
0	1.24 ± 0.02	0.62 ± 0.01
1	1.23 ± 0.02	0.62 ± 0.01
2	1.25 ± 0.02	0.62 ± 0.01
3	1.27 ± 0.02	0.62 ± 0.01
5	1.26 ± 0.02	0.62 ± 0.01
25	1.24 ± 0.02	0.62 ± 0.01
50		0.63 ± 0.01
100	1.16 ± 0.02	0.64 ± 0.01

Network Structure in Carbon Black Filled Vulcanisates. The network structure in filled EPDM vulcanisates was studied by the NMR method to establish structure−properties relationships. The T_2 relaxation time for filled EPDM before and after vulcanization is shown in Table 6. There is no difference in T_2 between unfilled EPDM and samples containing a moderate fraction of carbon black. T_2 for the sample with the highest carbon black N550 content is slightly shorter than for the other samples. This decrease is related to restriction of chain mobility due to interactions with carbon black. The density of adsorption junctions, $1/2M_{ad}$, in the sample with the highest filler content is about 17 mmol/kg.

Vulcanization of the samples causes the T_2 value to be roughly halved. T_2 in the vulcanisates does not depend on the carbon black content. This suggests that the total network density, $1/2M_{c+e+ad}$, in all vulcanisates is the same. A value of $1/2M_{c+e+ad}$ is composed of chemical cross-links (c), chain entanglements (e), and EPDM−carbon black adsorption junctions (ad). $1/2M_{c+e+ad}$ equals about 430 mmol/kg for all samples studied. The density of chemical cross-links in the vulcanisates, $1/2M_c$, might be estimated from the value of $1/2M_{c+e+ad}$. If we assume that (i) chemical cross-links, chain entanglements, and adsorption junctions are decoupled and (ii) the entanglement density is independent of the carbon black content, the following equation is valid:

$$1/2M_{c+e+ad} = 1/2M_c + 1/2M_e + 1/2M_{ad} \qquad (9)$$

The total network density and contributions to its value from chemical cross-links, chain entanglements, and EPDM−carbon black adsorption junctions are given in Table 7 for the unfilled vulcanisate and the vulcanisate with the highest carbon black content. Figure 18A shows the network structure and microphase composition of the vulcanisate (N550/100 phr), as measured by the NMR method and extraction of the compound before vulcanization.

Mechanical Properties in Relation to the Reinforcement Effect of the Filler. In Table 8 the reinforcing factor of the filler as determined from the mechanical experiments is tabulated as a function of the fraction of carbon black in the various vulcanisates. In the glassy state (from the dynamic storage modulus

Table 7. Total Cross-Link Density (in mmol/kg) and the Contributions in $1/2M_{c+e+ad}$ from Chemical Cross-Links, Chain Entanglements, and EPDM/Carbon Black Adsorption Junctions for Unfilled Vulcanisate and Vulcanisate Filled with 100 wt Parts of Carbon Black N550[a]

sample	$1/2M_{c+e+ad}$	$1/2M_c$	$1/2M_e$	$1/2M_{ad}$
unfilled vulcanisate	430	165	265	0
filled vulcanisate	425	143	265	17

[a] The entanglement density of 265 mmol/kg for unfilled EPDM vulcanisate is taken for the calculation.[20]

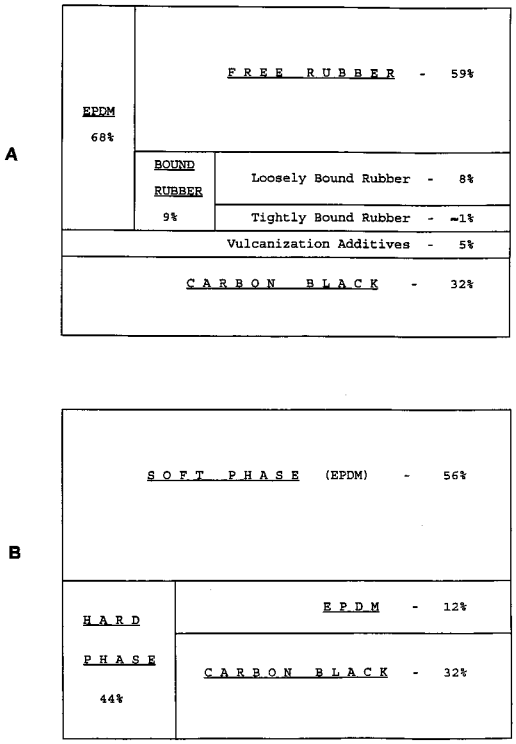

Figure 18. Structure of EPDM/N550 (phr = 100) vulcanisate according to NMR and extraction studies (A) and mechanical data for the case of pure hydrodynamic reinforcement (B). The volume fraction of microphases/components is given in percent. According to NMR data, the total network density in the rubber phase, $1/2M_{c+e+ad}$, is equal to 425 mmol/kg. The density of the adsorption junctions in the loosely bound rubber, $1/2M_{ad}$, is equal to 17 mmol/kg.

Table 8. Reinforcing Factor *f* of the Filler in the Vulcanized Carbon Black Filled Samples as a Function of the Amount of Carbon Black N550

parts CB phr	volume fraction	*f*(vulc) from *E′*(*T*) *T* = −75 °C	*f*(vulc) from M−R *T* = 30 °C	*f*(vulc) from *E′*(*T*) *T* = 30 °C
2	0.0089	0.99 ± 0.05	1.01 ± 0.05	1.02 ± 0.05
5	0.022	1.09 ± 0.05	1.09 ± 0.05	1.12 ± 0.05
25	0.101	1.29 ± 0.05	1.69 ± 0.05	2.0 ± 0.2
50	0.183	1.50 ± 0.05	2.71 ± 0.05	5.8 ± 0.5
100	0.309	2.01 ± 0.05	6.52 ± 0.05	23.8 ± 1.0

at −75 °C) the reinforcing factor of the filler is the lowest. From the high-strain Mooney-Rivlin experiments at room temperature it is observed that the filler particles are much more effective in reinforcing the material, especially at higher filler contents (≥25 phr of carbon black N550). Finally, the filler particles show the largest reinforcing effect in the low-strain rubbery modulus (from the dynamic storage modulus at 30 °C). For the sample filled with 100 phr of carbon black, the rubbery modulus increases about 24-fold due to the filler particles, while the glassy modulus increases only 2-fold.

Following the analysis by Eggers,[55] the empirical Thomas equation is used to predict the reinforcement factor (*f*) as a function of the filler volume fraction (φ):

$$f(\varphi) = 1 + 2.5\varphi + 10.05\varphi^2 + 0.00273 \exp(16.6\varphi) \quad (10)$$

It appears that the reinforcement factors determined from dynamic measurements in the glassy state are within experimental accuracy in agreement with the predictions according to the Thomas equation, as are the reinforcing factor in and the rubbery state for the samples with 2 and 5 phr of carbon black. By contrast, the Mooney-Rivlin and dynamic storage modulus results for the samples filled with 25, 50, and 100 parts of carbon black deviate significantly from the predictions.

Several reinforcing mechanisms have been suggested in the literature by many authors: (i) a hydrodynamic effect due to the volume occupied by the carbon black particles, with possible voids in the carbon black-aggregates and a nonspherical shape of the filler;[55] (ii) the formation of a layer of bound rubber at the surface of the carbon black particles;[55,56] (iii) the formation of an elastically active network of carbon black particles.[56]

As discussed by Huber et al.,[56] all three mechanisms are expected to contribute to the small strain rubbery modulus as determined with the aid of dynamic mechanical experiments at 30 °C. The combined action of these three mechanisms results in a large reinforcing factor (*f*) of the filler particles, especially for the samples filled with 50 and 100 phr carbon black. The reinforcing increases as the EPDM−carbon black interfacial area per unit volume EPDM increases, as can be seen from Figure 19.

Elastically active networks of carbon black particles are known to be deformation sensitive.[56] At high strains the interactions between the particles are broken. Therefore, such a network, if present, does not contribute to the Mooney-Rivlin results, and intermediate values for the reinforcing factor (*f*) are found. From these values the volume fraction of the hard phase, i.e., carbon black particles with a layer of bound rubber, may be estimated using the Thomas equation. A reinforcing factor of 6.5, as found for the sample with 100 phr of carbon black, suggests that the total volume faction of the hard phase is about 44%. Thus, with 32 vol% carbon black, the volume fraction of the bound layer amounts to about 12%, as shown in Figure 18. It is assumed that the vulcanization additives reside in the rubbery phase. The obtained volume fraction of the soft phase is in good agreement with the picture that arises from the NMR experiment on the reinforcing effect of carbon black with respect to the hard/soft phase composition. Finally, the stiffness of a possible layer of bound layer equals the stiffness of vitrified rubber. Therefore, such layer if present will not affect the glassy modulus as determined with dynamic mechanical analysis at −75 °C. The reinforcing effect of the CB particles is only due to hydrodynamic effects. For the materials studied these can, within experimental accuracy, be described with the Thomas equation, suggesting that the filler particles are well dispersed and have a spherical shape.

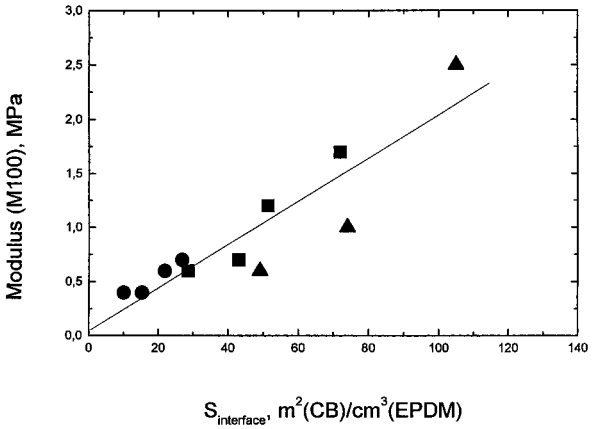

Figure 19. Retractive force at 100% elongation versus the maximum possible EPDM−carbon black contact area per unit volume of the elastomer, $\Psi = \varphi\rho S_{sp}/(1 - \varphi)$, in compounds filled with different types of carbon black. The symbols used in this figure correspond to the ones of Figure 7. The line is a guide to the eye.

Conclusions

Proton T_2 relaxation experiments were used to study the EPDM/carbon black interface. It was shown that two microregions with significantly different local chain mobility are observed in the filled EPDM: a thin layer of immobilized (semirigid) EPDM chain units covering the surface of the carbon black and a mobile (viscoelastic) EPDM matrix outside of the EPDM/carbon black interface. The thickness of the interfacial layer is in the range of one to two diameters of the monomer unit (≈1 nm). The interface provides adsorption junctions at the sites of interaction between the carbon black and the EPDM. These junctions interconnect the neighboring carbon black particles and aggregates. It has been shown that a spatially heterogeneous, "bimodal"-like distribution of the adsorption junctions provides a good representation of the structure of the physical network in the rubber matrix. One fraction of the EPDM matrix, *the loosely bound rubber*, has numerous adsorption interactions with the surface of the carbon black, similar to the interactions in the bound rubber. The other fraction of the EPDM, *the unbound rubber*, has a relatively low number of adsorption network junctions and can therefore be extracted from the compounds. The fraction of the loosely bound rubber increases as the EPDM−carbon black contact area per unit volume of the elastomer increases and is rather close to the content of bound rubber, regardless of the type of carbon black.

Mechanical experiments reveal that several factors contribute to the reinforcing effect of the filler. The effect of adsorption junctions increases as the EPDM−carbon black interfacial area per unit volume of the EPDM increases.

Acknowledgment. It is a pleasure to acknowledge the assistance of J. Koen, C. Raemaekers, and S. Sheiko in the acquisition and analysis of transmission light microscopy, TGA-MS and AFM data, respectively. The author greatly appreciates Dr. W. Barendswaard's helpful discussions and comments on the manuscript. The carbon black and its characterization were kindly provided by Dr. M. Smith from Cabot B.V., Leiden, NL.

References and Notes

(1) Kraus, G. In *Reinforcement of Elastomers*; Wiley: New York, 1965.
(2) Donnet, J. B.; Voet, A. *Carbon Black Physics, Chemistry and Elastomer Reinforcement*; Marcel Dekker: New York, 1976.
(3) Rigbi, Z. *Adv. Polym. Sci.* **1980**, *36*, 21.
(4) Danneberg, E. M. *Rubber Chem. Technol.* **1975**, *48*, 410.
(5) Donnet, J. B.; Vidal, A. *Adv. Polym. Sci.* **1986**, *76*, 103.
(6) Edwards, D. C. *J. Mater. Sci.* **1990**, *25*, 4175.
(7) Donnet, J. B. *Kautsch. Gummi Kunstst.* **1992**, *45*, 459; **1994**, *47*, 628.
(8) Wolf, S.; Wang, M. J.; Tan, E. H. *Kautsch. Gummi Kunstst.* **1994**, *47*, 780; **1994**, *47*, 873.
(9) Gerspacher, M. G.; O'Farrell, C. P. *Kautsch. Gummi Kunstst.* **1992**, *45*, 97. Gerspacher, M. G.; O'Farrell, C. P.; Yang, H. H. *Kautsch. Gummi Kunstst.* **1994**, *47*, 349.
(10) Danneberg, E. M. *Prog. Rubber Plast. Technol.* **1985**, *1*, 13.
(11) Pliskin, I.; Tokita, N. *J. Appl. Polym. Sci.* **1972**, *16*, 473.
(12) Danneberg, E. M. *Rubber Chem. Technol.* **1986**, *59*, 512.
(13) Litvinov, V. M. In *Organosilicon Chemistry: From Molecules to Materials II*; Auner, N., Weis, J., Eds.; VCH: Weinheim, 1996; p 779 and references therein.
(14) McBrierty, V. J.; Kenny, J. C. *Kautsch. Gummi Kunstst.* **1994**, *47*, 342 and references therein.
(15) Gotlib, Yu. Y.; Lifshits, M. I.; Shevelev, V. A.; Lishanskii, I. A.; Balanina, I. V. *Polym. Sci., USSR* **1986**, *18*, 2630.
(16) Simon, G.; Baumann, K.; Gronski, W. *Macromolecules* **1992**, *25*, 3624.
(17) Simon, G.; Birnstiel, A.; Schimmel, H.-H. *Polym. Bull.* **1989**, *21*, 235.
(18) Litvinov, V. M.; Vasil'ev, V. G. *Polym. Sci. USSR* **1990**, *32*, 2231.
(19) Gasilova, Ye. R.; Shevelev, V. A. *Polym. Sci. USSR* **1989**, *31*, 1683.
(20) Litvinov, V. M.; Barendswaard, W.; van Duin, M. *Rubber Chem. Technol.* **1998**, *71*, 105.
(21) Booij, H. C. *Kautsch. Gummi Kunstst.* **1991**, *44*, 128.
(22) Leblanc, J. L.; Hardy, P. *Kautsch. Gummi Kunstst.* **1991**, *44*, 1119.
(23) Wang, M.-J.; Wolff, S.; Tan, E.-H. *Rubber Chem. Technol.* **1993**, *66*, 178.
(24) Cohen-Addad, J. P.; Dupeyre, R. *Polymer* **1983**, *24*, 400.
(25) Press: W. H.; Flannery, B. P.; Teukolsky, S. A.; Vetterling, T. *Numerical Recipes−The Art of Scientific Computing*; Cambridge University Press: Cambridge, 1986.
(26) Ferry, J. D. *Viscoelastic Properties of Polymers*; John Wiley & Sons: New York, 1980.
(27) Treloar, L. R. G. *The Physics of Rubber Elasticity*; Oxford: New York, 1975.
(28) Cohen-Addad, J. P. *Progr. NMR Spectrosc.* **1993**, *25*, 1 and references therein.
(29) Charlesby, A. In *Radiation effects on Polymers*; Clough, R. L., Shalaby, S. W., Eds.; ACS Symposium Series; American Chemical Society: Washington, DC, 1991; Vol. 475, p 193 and references therein.
(30) Cohen-Addad, J. P.; Girard, O. *Macromolecules* **1992**, *25*, 593.
(31) Litvinov, V. M. *Int. Polym. Sci. Technol.* **1988**, *15*, T/28.
(32) Weber, H. W.; Kimmich, R. *Macromolecules* **1993**, *26*, 2597.
(33) Kimmich, R.; Köpf, M.; Callaghan, P. *J. Polym. Sci., Part B: Polym. Phys.* **1991**, *29*, 1025.
(34) Kulagina, T. P.; Litvinov, V. M.; Summanen, K. T. *J. Polym. Sci., Part B: Polym. Phys.* **1993**, *31*, 241.
(35) Sandakov, G. I.; Tarasov, V. P.; Volkova, N. N.; Ol'khov, Y. A.; Smirnov, L. P.; Erofeev, L. N.; Khitrin, A. K. *Vysokomol. Soedin., Ser. B* **1989**, *31*, 821.
(36) Volkova, N. N.; Sandakov, G. I.; Sosikov, A. I.; Ol'khov, Y. A.; Smirnov, L. P.; Summanen, K. T. *Polym. Sci. USSR* **1992**, *34*, 127.
(37) McBrierty, V. J.; Packer, K. J. *Nuclear Magnetic Resonance in Solid Polymers*; Cambridge University Press: Cambridge, 1993.
(38) Cashell, E. M.; Douglass, D. C.; McBrierty, V. J. *Polym. J.* **1978**, *10*, 557.
(39) Ren, W.; Veeman, W. S.; Litvinov, V. M., unpublished results.
(40) O'Brien, J.; Cashell, E.; Wardell, G. E.; McBrierty, V. J. *Macromolecules* **1976**, *9*, 653.
(41) Charlesby, A.; Jaroszkiewicz, E. M. *Eur. Polym. J.* **1985**, *21*, 55.
(42) Cohen-Addad, J. P.; Morel, N. *J. Phys. III* **1996**, *6*, 267.
(43) Cohen-Addad, J. P.; Frébourg, P. *Polymer* **1996**, *37*, 4235.
(44) Boyer, R. F.; Miller, R. L. *Macromolecules* **1977**, *10*, 1167.
(45) Sharaf, M. A.; Kloczkowski, A.; Mark, J. E. *Comput. Polym. Sci.* **1994**, *4*, 29.
(46) Cohen-Addad, J. P. *Polymer* **1989**, *30*, 1820.
(47) Meissner, B. *J. Appl. Polym. Sci.* **1993**, *50*, 285 and references therein.
(48) Richter, D.; Farago, B.; Butera, R.; Fetters, L. J.; Huang, J. S.; Ewen, B. *Macromolecules* **1993**, *26*, 6, 795.
(49) Lodge, T. P.; Rotstein, N. A.; Prager, S. In *Advances in Chemical Physics*; Prigogine, I., Rice, S. A, Eds.; Wiley: New York, 1990; Vol. 79, p 1.
(50) Kimmich, R.; Schnur, G.; Köpf, M. *Prog. NMR Spectrosc.* **1988**, *20*, 385 and references therein.
(51) Cuniberti, C. *J. Polym. Sci., Part A-2* **1970**, *8*, 2051.
(52) Cohen-Addad, J. P.; Marchand, J. P.; Viallat, A. *Polymer* **1994**, *35*, 1629.
(53) Schmit, C.; Cohen-Addad, J. P. *Macromolecules* **1989**, *22*, 142.
(54) Leblanc, J. L. *Prog. Rubber Plastics Technol.* **1994**, *10*, 112.
(55) Eggers, H.; Schümmer, P. *Rubber Chem. Technol.* **1996**, *69*, 253.
(56) Huber, G.; Vilgis, T. A. *Kautsch. Gummi Kunstst.* **1999**, *52*, 102.

MA9910080